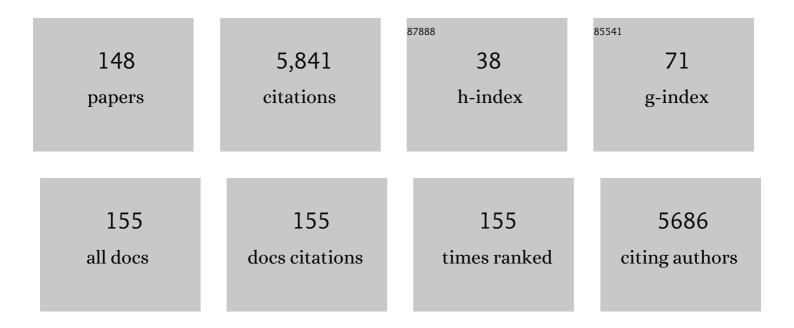
## **Robin S Shandas**

List of Publications by Year in descending order

Source: https://exaly.com/author-pdf/6928493/publications.pdf Version: 2024-02-01



#	Article	IF	CITATIONS
1	Injectable Polymeric Delivery System for Spatiotemporal and Sequential Release of Therapeutic Proteins To Promote Therapeutic Angiogenesis and Reduce Inflammation. ACS Biomaterials Science and Engineering, 2020, 6, 1217-1227.	5.2	28
2	An injectable sulfonated reversible thermal gel for therapeutic angiogenesis to protect cardiac function after a myocardial infarction. Journal of Biological Engineering, 2019, 13, 6.	4.7	19
3	Gold Nanoparticle-Functionalized Reverse Thermal Gel for Tissue Engineering Applications. ACS Applied Materials & Interfaces, 2019, 11, 18671-18680.	8.0	47
4	Microgrooves Encourage Endothelial Cell Adhesion and Organization on Shape-Memory Polymer Surfaces. ACS Applied Bio Materials, 2019, 2, 1897-1906.	4.6	11
5	Structural and Biomechanical Adaptations of Right Ventricular Remodeling—In Pulmonary Arterial Hypertension—Reduces Left Ventricular Rotation During Contraction: A Computational Study. Journal of Biomechanical Engineering, 2019, 141, .	1.3	9
6	Measurement of Wall Shear Stress Exerted by Flowing Blood in the Human Carotid Artery: Ultrasound Doppler Velocimetry and Echo Particle Image Velocimetry. Ultrasound in Medicine and Biology, 2018, 44, 1392-1401.	1.5	34
7	Development of an electrospun biomimetic polyurea scaffold suitable for vascular grafting. Journal of Biomedical Materials Research - Part B Applied Biomaterials, 2018, 106, 278-290.	3.4	10
8	A sulfonated reversible thermal gel for the spatiotemporal control of VEGF delivery to promote therapeutic angiogenesis. Journal of Biomedical Materials Research - Part A, 2018, 106, 3053-3064.	4.0	15
9	Left ventricular torsion rate and the relation to right ventricular function in pediatric pulmonary arterial hypertension. Pulmonary Circulation, 2018, 8, 1-10.	1.7	10
10	Echo Particle Image Velocimetry for Estimation of Carotid Artery Wall Shear Stress: Repeatability, Reproducibility and Comparison with Phase-Contrast Magnetic Resonance Imaging. Ultrasound in Medicine and Biology, 2017, 43, 1618-1627.	1.5	16
11	Injectable Carbon Nanotube-Functionalized Reverse Thermal Gel Promotes Cardiomyocytes Survival and Maturation. ACS Applied Materials & Interfaces, 2017, 9, 31645-31656.	8.0	52
12	Circulating miRNAs in Pediatric Pulmonary Hypertension Show Promise as Biomarkers of Vascular Function. Oxidative Medicine and Cellular Longevity, 2017, 2017, 1-11.	4.0	16
13	Shape Memory Polymers Containing Higher Acrylate Content Display Increased Endothelial Cell Attachment. Polymers, 2017, 9, 572.	4.5	7
14	A Zero-Dimensional Model and Protocol for Simulating Patient-Specific Pulmonary Hemodynamics From Limited Clinical Data. Journal of Biomechanical Engineering, 2016, 138, .	1.3	7
15	Analysis of pediatric airway morphology using statistical shape modeling. Medical and Biological Engineering and Computing, 2016, 54, 899-911.	2.8	8
16	Biomimetic Polymers for Cardiac Tissue Engineering. Biomacromolecules, 2016, 17, 1593-1601.	5.4	37
17	Main Pulmonary Arterial Wall Shear Stress Correlates with Invasive Hemodynamics and Stiffness in Pulmonary Hypertension. Pulmonary Circulation, 2016, 6, 37-45.	1.7	48
18	Vorticity is a Marker of Diastolic Ventricular Interdependency in Pulmonary Hypertension. Pulmonary Circulation, 2016, 6, 46-54.	1.7	26

#	Article	IF	CITATIONS
19	Characterization of CMR-derived haemodynamic data in children with pulmonary arterial hypertension. European Heart Journal Cardiovascular Imaging, 2016, 18, jew152.	1.2	24
20	4D magnetic resonance flow imaging for estimating pulmonary vascular resistance in pulmonary hypertension. Journal of Magnetic Resonance Imaging, 2016, 44, 914-922.	3.4	34
21	Non-invasive determination by cardiovascular magnetic resonance of right ventricular-vascular coupling in children and adolescents with pulmonary hypertension. Journal of Cardiovascular Magnetic Resonance, 2015, 17, 81.	3.3	31
22	Assessment of Nâ€Terminal Prohormone Bâ€Type Natriuretic Peptide as a Measure of Vascular and Ventricular Function in Pediatric Pulmonary Arterial Hypertension. Pulmonary Circulation, 2015, 5, 658-666.	1.7	10
23	A heparinâ€mimicking reverse thermal gel for controlled delivery of positively charged proteins. Journal of Biomedical Materials Research - Part A, 2015, 103, 2102-2108.	4.0	17
24	Characterization of micro-invasive trabecular bypass stents by ex vivo perfusion and computational flow modeling. Clinical Ophthalmology, 2014, 8, 499.	1.8	37
25	Extubation force depends upon angle of force application and fixation technique: a study of 7 methods. BMC Anesthesiology, 2014, 14, 74.	1.8	14
26	The design and fabrication of two portal vein flow phantoms by different methods. Medical Physics, 2014, 41, 023701.	3.0	5
27	Biocompatibility and tissue integration of a novel shape memory surgical mesh for ventral hernia: In vivo animal studies. Journal of Biomedical Materials Research - Part B Applied Biomaterials, 2014, 102, 1093-1100.	3.4	12
28	A Survey of Surface Modification Techniques for Next-Generation Shape Memory Polymer Stent Devices. Polymers, 2014, 6, 2309-2331.	4.5	71
29	Hydrogel formulation determines cell fate of fetal and adult neural progenitor cells. Stem Cell Research, 2014, 12, 11-23.	0.7	31
30	A Novel Microfluidic Chip for Assessing Dynamic Adhesion Behavior of Cell-Targeting Microbubbles. Ultrasound in Medicine and Biology, 2014, 40, 148-157.	1.5	8
31	Mesoporous silica nanoparticles as a breast-cancer targeting ultrasound contrast agent. Colloids and Surfaces B: Biointerfaces, 2014, 116, 652-657.	5.0	107
32	Patient-Specific Imaging-Based Techniques for Optimization of Pediatric Cardiovascular Surgery. , 2014, , 3471-3490.		0
33	Wall shear stress measured by phase contrast cardiovascular magnetic resonance in children and adolescents with pulmonary arterial hypertension. Journal of Cardiovascular Magnetic Resonance, 2013, 15, 81.	3.3	57
34	Paclitaxel-liposome–microbubble complexes as ultrasound-triggered therapeutic drug delivery carriers. Journal of Controlled Release, 2013, 166, 246-255.	9.9	213
35	An investigation of industrial molding compounds for use in 3D ultrasound, MRI, and CT imaging phantoms. Medical Physics, 2013, 40, 052905.	3.0	15
36	High pulsatility flow stimulates smooth muscle cell hypertrophy and contractile protein expression. American Journal of Physiology - Lung Cellular and Molecular Physiology, 2013, 304, L70-L81.	2.9	49

#	Article	IF	CITATIONS
37	Fabrication and Characterization of Novel High Modulus, Two-Stage Reactive Thiol-Acrylate Composite Polymer Systems. Macromolecular Symposia, 2013, 329, 101-107.	0.7	13
38	Integrating a novel shape memory polymer into surgical meshes decreases placement time in laparoscopic surgery: An <i>in vitro</i> and acute <i>in vivo</i> study. Journal of Biomedical Materials Research - Part A, 2013, 101A, 2613-2620.	4.0	16
39	Influence of Distal Resistance and Proximal Stiffness on Hemodynamics and RV Afterload in Progression and Treatments of Pulmonary Hypertension: A Computational Study with Validation Using Animal Models. Computational and Mathematical Methods in Medicine, 2013, 2013, 1-12.	1.3	16
40	A Novel Cationic Microbubble Coated with Stearic Acid-Modified Polyethylenimine to Enhance DNA Loading and Gene Delivery by Ultrasound. PLoS ONE, 2013, 8, e76544.	2.5	29
41	Mechanics and Function of the Pulmonary Vasculature: Implications for Pulmonary Vascular Disease and Right Ventricular Function. , 2012, 2, 295-319.		61
42	Ultrasonic Imaging of Endothelial CD81 Expression Using CD81-Targeted Contrast Agents in InÂVitro and InÂVivo Studies. Ultrasound in Medicine and Biology, 2012, 38, 670-680.	1.5	16
43	Impact of pulmonary vascular stiffness and vasodilator treatment in pediatric pulmonary hypertension: 21 patient-specific fluid–structure interaction studies. Computer Methods and Programs in Biomedicine, 2012, 108, 617-628.	4.7	18
44	A new flow co-culture system for studying mechanobiology effects of pulse flow waves. Cytotechnology, 2012, 64, 649-666.	1.6	20
45	Two‣tage Reactive Polymer Network Forming Systems. Advanced Functional Materials, 2012, 22, 1502-1510.	14.9	127
46	Development of a Minimally Invasive, Injectable, Shape Memory Suture and Delivery System. Annals of Biomedical Engineering, 2012, 40, 1520-1529.	2.5	10
47	Impact of Residual Stretch and Remodeling on Collagen Engagement in Healthy and Pulmonary Hypertensive Calf Pulmonary Arteries at Physiological Pressures. Annals of Biomedical Engineering, 2012, 40, 1419-1433.	2.5	20
48	Enhanced two-stage reactive polymer network forming systems. Polymer, 2012, 53, 2429-2434.	3.8	38
49	Pulmonary Vascular Stiffness: Measurement, Modeling, and Implications in Normal and Hypertensive Pulmonary Circulations. , 2011, 1, 1413-1435.		43
50	Microstructural Changes in Collagen and Elastin and Their Impact on the Mechanics of the Pulmonary Artery in Hypertension. , 2011, , .		0
51	In Vitro and Preliminary In Vivo Validation of Echo Particle Image Velocimetry in Carotid Vascular Imaging. Ultrasound in Medicine and Biology, 2011, 37, 450-464.	1.5	84
52	Real-Time Texture Analysis for Identifying Optimum Microbubble Concentration in 2-D Ultrasonic Particle Image Velocimetry. Ultrasound in Medicine and Biology, 2011, 37, 1280-1291.	1.5	19
53	A Microstructurally Driven Model for Pulmonary Artery Tissue. Journal of Biomechanical Engineering, 2011, 133, 051002.	1.3	32
54	Linked opening angle and histological and mechanical aspects of the proximal pulmonary arteries of healthy and pulmonary hypertensive rats and calves. American Journal of Physiology - Heart and Circulatory Physiology, 2011, 301, H1810-H1818.	3.2	14

#	Article	IF	CITATIONS
55	Nucleus Replacement Device Failure. Spine, 2010, 35, E1241-E1247.	2.0	12
56	Conduit Arteries In The Rat And Calf Express Different Material Property Changes In Response To Hypoxia-Induced Pulmonary Hypertension. , 2010, , .		1
57	Quantification of Hemodynamic Wall Shear Stress in Patients with Bicuspid Aortic Valve Using Phase-Contrast MRI. Annals of Biomedical Engineering, 2010, 38, 788-800.	2.5	163
58	Effects of thermal rates on the thermomechanical behaviors of amorphous shape memory polymers. Mechanics of Time-Dependent Materials, 2010, 14, 219-241.	4.4	75
59	Computational simulation of the pulmonary arteries and its role in the study of pediatric pulmonary hypertension. Progress in Pediatric Cardiology, 2010, 30, 63-69.	0.4	16
60	Photopolymerized thiol-ene systems as shape memory polymers. Polymer, 2010, 51, 4383-4389.	3.8	124
61	In vivo measurement of proximal pulmonary artery elastic modulus in the neonatal calf model of pulmonary hypertension: development and ex vivo validation. Journal of Applied Physiology, 2010, 108, 968-975.	2.5	42
62	Measurement uncertainty in pulmonary vascular input impedance and characteristic impedance estimated from pulsed-wave Doppler ultrasound and pressure: clinical studies on 57 pediatric patients. Physiological Measurement, 2010, 31, 729-748.	2.1	6
63	Direct echo PIV flow vector mapping on ultrasound DICOM images. , 2010, , .		1
64	Effect of Vessel Stiffening and High Pulsatility Flow on Contractile Function and Proliferation of Small Arterial Cells. , 2010, , .		0
65	Constitutive Modeling of Anisotropic Finite-Deformation Hyperelastic Behaviors of Soft Materials Reinforced by Tortuous Fibers. , 2010, 2, 19-29.		1
66	In Vivo Validation of Echo Partical Image Velocimetry (Echo PIV) in Human Carotid Arteries Using Phase-Contrast MRI. , 2009, , .		2
67	Wave scattering from encapsulated microbubbles subject to high-frequency ultrasound: Contribution of higher-order scattering modes. Journal of the Acoustical Society of America, 2009, 126, 1766-1775.	1.1	9
68	Effects of Pathological Flow on Pulmonary Artery Endothelial Production of Vasoactive Mediators and Growth Factors. Journal of Vascular Research, 2009, 46, 561-571.	1.4	63
69	Influence of Distal Resistance and Proximal Vascular Stiffness on Vascular Impedance and Hemodynamics in Pulmonary Hypertension: A Computational Study With Validation Using an Animal Model. , 2009, , .		Ο
70	High Pulsatility Flow Induces Adhesion Molecule and Cytokine mRNA Expression in Distal Pulmonary Artery Endothelial Cells. Annals of Biomedical Engineering, 2009, 37, 1082-1092.	2.5	93
71	Capacitive micromachined ultrasonic transducers using commercial multi-user MUMPs process: Capability and limitations. Ultrasonics, 2009, 49, 765-773.	3.9	18
72	An Artificial Right Ventricle for Failing Fontan: In Vitro and Computational Study. Annals of Thoracic Surgery, 2009, 88, 170-176.	1.3	56

#	Article	IF	CITATIONS
73	Quantification of Elastin Residual Stretch in Fresh Artery Tissue: Impact on Artery Material Properties and Pulmonary Hypertension Pathophysiology. , 2009, , .		0
74	Measurement of Valve Lesion Morphology and Aorta / Flow-Jet Patterns in Bicuspid Aortic Valve Patients. , 2009, , .		0
75	Strong, Tailored, Biocompatible Shapeâ€Memory Polymer Networks. Advanced Functional Materials, 2008, 18, 2428-2435.	14.9	321
76	Finite deformation thermo-mechanical behavior of thermally induced shape memory polymers. Journal of the Mechanics and Physics of Solids, 2008, 56, 1730-1751.	4.8	357
77	Noninvasive Methods for Determining Pulmonary Vascular Function in Children with Pulmonary Arterial Hypertension: Application of a Mechanical Oscillator Model. Congenital Heart Disease, 2008, 3, 106-116.	0.2	6
78	Pulmonary vascular input impedance is a combined measure of pulmonary vascular resistance and stiffness and predicts clinical outcomes better than pulmonary vascular resistance alone in pediatric patients with pulmonary hypertension. American Heart Journal, 2008, 155, 166-174.	2.7	142
79	Changes in the structure-function relationship of elastin and its impact on the proximal pulmonary arterial mechanics of hypertensive calves. American Journal of Physiology - Heart and Circulatory Physiology, 2008, 295, H1451-H1459.	3.2	127
80	Systematic validation of the echo particle image velocimetry technique using a patient specific carotid bifurcation model. , 2008, , .		2
81	Development of a custom-designed echo particle image velocimetry system for multi-component hemodynamic measurements: system characterization and initial experimental results. Physics in Medicine and Biology, 2008, 53, 1397-1412.	3.0	58
82	Validation of a Second-Generation Echo PIV System in Patient-Specific Carotid Artery Models: In Vitro Studies Using Pulsatile Flow. , 2008, , .		0
83	Effect of Vascular Stiffness on Pulmonary Flow in Normotensive and Hypertensive States: Numerical Study With Fluid Structure Interaction. , 2008, , .		0
84	Abstract 4388: In-Vivo Pulmonary Vascular Stiffness Obtained from Color M-Mode Tissue Doppler Imaging and Pressure Measurements Predicts Clinical Outcomes Better than Indexed Pulmonary Vascular Resistance in Pediatric Patients with Pulmonary Arterial Hypertension. Circulation, 2008, 118,	1.6	3
85	Application of A Microstructural Constitutive Model of the Pulmonary Artery to Patient-Specific Studies: Validation and Effect of Orthotropy. Journal of Biomechanical Engineering, 2007, 129, 193-201.	1.3	18
86	Thermomechanical indentation of shape memory polymers. , 2007, , .		2
87	Comparison of mechanical behavior among the extrapulmonary arteries from rats. Journal of Biomechanics, 2007, 40, 812-819.	2.1	18
88	Computational fluid dynamics analysis of microbubble formation in microfluidic flow-focusing devices. Microfluidics and Nanofluidics, 2007, 3, 195-206.	2.2	36
89	Unconstrained recovery characterization of shape-memory polymer networks for cardiovascular applications. Biomaterials, 2007, 28, 2255-2263.	11.4	536
90	A Comparative Study of Mechanical Properties of Fresh and Elastic-Network Only Proximal Artery Tissues. , 2007, , .		0

#	Article	IF	CITATIONS
91	An Implantable Transit-Time Aortic Flow Probe Using Capacitive Micromachined Ultrasound Transducers: Design and Optimization. , 2007, , .		0
92	Patient-Specific Fluid Structure Interaction Simulation Applied to Evaluating Hemodynamics Within the Total Cavopulmonary Connection. , 2007, , .		0
93	Real-Time Measurement of Multi-Component Velocity Vectors Within Abdominal Aortic Aneurysms Using Echo PIV: Comparison of In Vitro and Computational Results. , 2007, , .		0
94	Use of Cardiac Phase-Contrast MRI to Examine Hemodynamics and Wall Deformation Within the Aortic Root for Patients With Bicuspid Aortic Valves. , 2007, , .		0
95	Measurement of In-Vivo Pulmonary Vascular Impedance in Two Animal Models of Pulmonary Hypertension. , 2007, , .		0
96	Addition of Particle Tracking Techniques to Improve Two-Dimensional Echo PIV for Opaque Flow Measurement. , 2007, , .		0
97	Contribution of Elastin to the Mechanical Properties of Arterial Tissues. , 2007, , .		0
98	Use of Myocardial Performance Index in Pediatric Patients with Idiopathic Pulmonary Arterial Hypertension. Journal of the American Society of Echocardiography, 2006, 19, 21-27.	2.8	57
99	Noninvasive Doppler Tissue Measurement of Pulmonary Artery Compliance in Children with Pulmonary Hypertension. Journal of the American Society of Echocardiography, 2006, 19, 403-412.	2.8	48
100	Initial Experience With the Development and Numerical and In Vitro Studies of A Novel Low-Pressure Artificial Right Ventricle for Pediatric Fontan Patients. ASAIO Journal, 2006, 52, 682-692.	1.6	20
101	Efficiency differences in computational simulations of the total cavo-pulmonary circulation with and without compliant vessel walls. Computer Methods and Programs in Biomedicine, 2006, 81, 220-227.	4.7	18
102	Simulations of Congenital Septal Defect Closure and Reactivity Testing in Patient-Specific Models of the Pediatric Pulmonary Vasculature: A 3D Numerical Study With Fluid-Structure Interaction. Journal of Biomechanical Engineering, 2006, 128, 564-572.	1.3	40
103	Theoretical predictions of harmonic generation from submicron ultrasound contrast agents for nonlinear biomedical ultrasound imaging. Physics in Medicine and Biology, 2006, 51, 557-573.	3.0	21
104	Predicting backscatter characteristics from micron- and submicron-scale ultrasound contrast agents using a size-integration technique. IEEE Transactions on Ultrasonics, Ferroelectrics, and Frequency Control, 2006, 53, 639-644.	3.0	19
105	Real time multicomponent echo particle image velocimetry technique for opaque flow imaging. Applied Physics Letters, 2006, 88, 261915.	3.3	69
106	Tailored Nanoscale Contrast Agents for Magnetic Resonance Imaging. , 2005, , 581.		0
107	Thermomechanics of the shape memory effect in polymers for biomedical applications. Journal of Biomedical Materials Research - Part A, 2005, 73A, 339-348.	4.0	301
108	Computational simulations of the total cavo-pulmonary connection: insights in optimizing numerical solutions. Medical Engineering and Physics, 2005, 27, 135-146.	1.7	26

#	Article	IF	CITATIONS
109	Advantages in using multifrequency excitation of contrast microbubbles for enhancing echo particle image velocimetry techniques: Initial numerical studies using rectangular and triangular waves. Ultrasound in Medicine and Biology, 2005, 31, 99-108.	1.5	35
110	A Microstructural Hyperelastic Model of Pulmonary Arteries Under Normo- and Hypertensive Conditions. Annals of Biomedical Engineering, 2005, 33, 1042-1052.	2.5	43
111	Aortic Input Impedance Increases With Age in Healthy Men and Women. Hypertension, 2005, 45, 1101-1106.	2.7	20
112	Free Recovery Effects of Shape-Memory Polymers for Cardiovascular Stents. Materials Research Society Symposia Proceedings, 2005, 898, 1.	0.1	1
113	Optimizing the Thermomechanics of Shape-Memory Polymers for Biomedical Applications. Materials Research Society Symposia Proceedings, 2004, 855, 99.	0.1	0
114	Extraction of Pulmonary Vascular Compliance, Pulmonary Vascular Resistance, and Right Ventricular Work From Single-Pressure and Doppler Flow Measurements in Children With Pulmonary Hypertension: a New Method for Evaluating Reactivity. Circulation, 2004, 110, 2609-2617.	1.6	69
115	Characterizing Vortex Ring Behavior During Ventricular Filling with Doppler Echocardiography: An in Vitro Study. Annals of Biomedical Engineering, 2004, 32, 245-256.	2.5	34
116	Noninvasive Measurement of Steady and Pulsating Velocity Profiles and Shear Rates in Arteries Using Echo PIV: In Vitro Validation Studies. Annals of Biomedical Engineering, 2004, 32, 1067-1076.	2.5	61
117	Development and validation of echo PIV. Experiments in Fluids, 2004, 36, 455-462.	2.4	167
118	Numerical modeling of microbubble backscatter to optimize ultrasound particle image velocimetry imaging: initial studies. Ultrasonics, 2004, 42, 1111-1121.	3.9	36
119	Dynamic three-dimensional reconstruction and modeling of cardiovascular anatomy in children with congenital heart disease using biplane angiography. Biomedical Sciences Instrumentation, 2004, 40, 200-5.	0.2	6
120	Stress and strain in rat pulmonary artery material during a biaxial bubble test. Biomedical Sciences Instrumentation, 2004, 40, 303-8.	0.2	3
121	Comparison of In Vitro Velocity Measurements in a Scaled Total Cavopulmonary Connection with Computational Predictions. Annals of Biomedical Engineering, 2003, 31, 810-822.	2.5	26
122	Insights into the effect of aortic compliance on Doppler diastolic flow patterns seen in coarctation of the aorta: A numeric study. Journal of the American Society of Echocardiography, 2003, 16, 162-169.	2.8	26
123	Influence of Connection Geometry and SVC-IVC Flow Rate Ratio on Flow Structures within the Total Cavopulmonary Connection: A Numerical Study. Journal of Biomechanical Engineering, 2002, 124, 364-377.	1.3	52
124	Use of intravascular ultrasound to measure local compliance of the pediatric pulmonary artery: In vitro studies. Journal of the American Society of Echocardiography, 2002, 15, 1507-1514.	2.8	15
125	Effect of Vessel Size on the Flow Efficiency of the Total Cavopulmonary Connection: In Vitro Studies. Pediatric Cardiology, 2002, 23, 171-177.	1.3	17
126	Reverse flow in compliant vessels and its implications for the Fontan procedure: numerical studies. Biomedical Sciences Instrumentation, 2002, 38, 321-6.	0.2	6

#	Article	IF	CITATIONS
127	Development of A Noninvasive Ultrasound Color M-Mode Means of Estimating Pulmonary Vascular Resistance in Pediatric Pulmonary Hypertension. Circulation, 2001, 104, 908-913.	1.6	48
128	Artificial Neural Network–Based Method of Screening Heart Murmurs in Children. Circulation, 2001, 103, 2711-2716.	1.6	132
129	Left Ventricular Filling Dynamics: Particle Image Velocimetry and Ultrasound Color M-Mode Imaging. , 2001, , .		0
130	Accuracy of the Bernoulli Equation for Estimation of Pressure Gradient Across Stenotic Blalock–Taussig Shunts: An In Vitro and Numerical Study. Pediatric Cardiology, 2000, 21, 439-447.	1.3	24
131	A Method for Determining the Reference Effective Flow Areas for Mechanical Heart Valve Prostheses. Circulation, 2000, 101, 1953-1959.	1.6	15
132	Pressure recovery and aortic stenosis. Journal of the American College of Cardiology, 2000, 35, 260.	2.8	0
133	Insights into catheter/doppler discrepancies in congenital aortic stenosis. American Journal of Cardiology, 1999, 83, 1447-1450.	1.6	18
134	Real-Time 3-Dimensional Volumetric Ultrasound Imaging of the Vena Contracta for Stenotic Valves with the Use of Echocardiographic Contrast Imaging: In Vitro Pulsatile Flow Studies. Journal of the American Society of Echocardiography, 1999, 12, 541-550.	2.8	7
135	Utility of Three-Dimensional Ultrasound Doppler Flow Reconstruction of the Proximal Jet to Quantify Effective Orifice Area: In Vitro Steady and Pulsatile Flow Studiesâ~†â~†â~tâ~â~â~ Journal of the American Soc Echocardiography, 1998, 11, 313-321.	ietzy.øf	27
136	Analysis of the Effect of Flow Rate on the Doppler Continuity Equation for Stenotic Orifice Area Calculations. Circulation, 1998, 97, 1597-1605.	1.6	71
137	Requirement for accurate measurement of regurgitant stroke volume by the combined continuous-wave Doppler and color Doppler flow convergence method. American Heart Journal, 1997, 133, 19-28.	2.7	7
138	Color flow Doppler determination of transmitral flow and orifice area in mitral stenosis: Experimental evaluation of the proximal flow-convergence method. American Heart Journal, 1995, 129, 114-123.	2.7	29
139	Nature of flow acceleration into a finite-sized orifice: Steady and pulsatile flow studies on the flow convergence region using simultaneous ultrasound Doppler flow mapping and laser Doppler velocimetry. Journal of the American College of Cardiology, 1995, 25, 1199-1212.	2.8	26
140	Factors influencing pulmonary venous flow velocity patterns in mitral regurgitation: An in vitro study. Journal of the American College of Cardiology, 1995, 26, 1333-1339.	2.8	16
141	Estimation of regurgitant flow volume based on centerline velocity/distance profiles using digital color M-Q Doppler: Application to orifices of different shapes. Journal of the American College of Cardiology, 1994, 24, 440-445.	2.8	21
142	Accuracy of flow convergence estimates of mitral regurgitant flow rates obtained by use of multiple color flow Doppler M-mode aliasing boundaries: An experimental animal study. American Heart Journal, 1993, 125, 449-458.	2.7	37
143	Cine magnetic resonance imaging and color Doppler flow mapping displays of flow velocity, spatial acceleration, and jet formation: A comparative in vitro study. American Heart Journal, 1993, 126, 1165-1173.	2.7	15
144	Effects of adjacent surfaces of different shapes on regurgitant jet sizes: An in vitro study using color Doppler imaging and laser-illuminated dye visualization. Journal of the American College of Cardiology, 1993, 22, 1522-1529.	2.8	15

#	Article	IF	CITATIONS
145	Experimental Studies to Define the Geometry of the Flow Convergence Region: Laser Doppler Particle Tracking and Color Doppler Imaging. Echocardiography, 1992, 9, 43-50.	0.9	48
146	Flow convergence calculations of flow rate through non or minimally restrictive orifices: In-vitro studies. Journal of the American College of Cardiology, 1991, 17, A359.	2.8	5
147	A new automatic computer method for measuring mean flow convergence radius from color MQ modes provides more accurate flow rate estimates: In-vitro and animal studies of mitral regurgitation. Journal of the American College of Cardiology, 1991, 17, A149.	2.8	9
148	Accuracy of flow convergence methods for calculating mitral regurgitant flow: Validation studies in an animal model. Journal of the American College of Cardiology, 1990, 15, A110.	2.8	12